

# Electric vehicles charging station configuration with closed loop control

Wisam Mohamed Najem, Omar Sh. Alyozbaky, Shaker M. Khudher

Department of Electrical Engineering, Faculty of Engineering, University of Mosul, Ninava, Iraq

---

## Article Info

### Article history:

Received May 4, 2022

Revised Sep 10, 2022

Accepted Oct 1, 2022

---

### Keywords:

Charging station

Electric vehicles

Grid to vehicle

LC filter

Micro-grid

---

## ABSTRACT

Recently, the demand for electric vehicles (EV) has been on the rise in global markets due to the orientation of national policies to reduce emissions and global warming through the electrification of the transportation sector and the use of clean energy sources. Electric vehicles function on batteries, which must be recharged, either by slow charging at home or by fast charging with a direct current. In the fast-charging process, the batteries can be charged in less than 15 minutes. In this paper, an off-board charger with a three-phase, six-pulse voltage rectifier was designed using the MATLAB/Simulink program. The closed control circuit was simulated, where the simulation results were influenced by changes to the input voltage. When the input voltage was increased or decreased by 5%, this control maintained the value of the current and voltage at the output to be equal to the reference values required to achieve fast charging. The simulation results showed that in the first case where no filter was used, the output voltage and current had a high amount of ripple that exceeded the permissible value. Therefore, a low-pass filter was designed to reduce the ripple factor to a value that was within the permissible limit.

*This is an open access article under the [CC BY-SA](https://creativecommons.org/licenses/by-sa/4.0/) license.*



---

## Corresponding Author:

Omar Sh. Alyozbaky

Department of Electrical Engineering, Faculty of Engineering, University of Mosul

Ninava, Iraq

Email: o.sh.alyozbaky@gmail.com

---

## 1. INTRODUCTION

Vehicles powered by fossil fuel are one of the main sources of gas emissions and environmental pollution, as well as global warming [1]–[3]. These emissions have led to severe climate change, which is reaching hazardous levels, as can be observed from the high degree of global warming and the melting of large icebergs. Therefore, preventive and precautionary measures must be taken to reduce these emissions. In this regard, the International Energy Agency (IEA) has identified certain scenarios for energy systems of the future in order to reduce the average rise in temperature by two degrees Celsius by 2050 [4]. One of the important scenarios is the use of clean energy sources, such as solar energy and wind energy, as well as the use of battery electric vehicles (BEVs). The use of electric energy in the transportation sector gives a better performance compared to the use of fuel because of its benefits in reducing emissions, as well as the use of electric motors that are characteristically highly efficient [5]. Although electric vehicles can contribute significantly to the reduction of global warming, vehicle drivers have fears with regard to their use because of the process of charging the batteries for their operation. That is why many researchers are now studying energy systems and developing the necessary solutions for the success of these vehicles. To alleviate the concern of vehicle drivers with regard to electric vehicles, focus is being given to the important issues of the development of charging technologies, battery designs and power system infrastructures, as well as moving

from slow-charging stations to fast-charging stations with a constant current in order to charge the batteries within a short period of time [6]. In addition, the economic and cost issues of electric cars are being studied, where the cost depends largely on the mechanism used in the technology for charging these vehicles to supply them with the required energy [7], [8]. The integration of electric vehicles into power systems has its pros and cons. Some of the disadvantages of adding electric vehicles to the electric network are the increasing load, the emergence of harmonics, the effect on the protection relays, the aging of transformers, insulators and cables, a decrease in the power factor, and a decrease in the voltage [9]–[14] on the positive side, it can be used to help the electrical network at peak times through vehicle-to-grid (V2G) technology [15].

A constant voltage and current are required to rapidly charge the batteries of electric vehicles. For this process, the alternating current needs to be converted to a direct current, and there are many configurations for achieving this. Power electronics devices are used in various configurations such as six or twelve pulses, three-phase or single-phase, controlled or uncontrolled. In uncontrolled rectifiers, the output voltage is governed by the input voltage. When the input voltage changes, so does the output voltage, and therefore, the output current will decrease or increase, thus affecting the charging [16]–[18]. For this reason, this research focused on developing this mechanism and using controlled rectifiers, that is, the output voltage can be controlled by controlling the pulses via a pulse generator to obtain the required output voltage [19]–[22].

In this paper, a three-phase charger with six pulses was designed. The charger was a controlled charger in order to obtain the output value based on the voltage required to charge the batteries of the electric vehicle. Also, to get the best performance and a constant output current and voltage, a closed loop system was designed for the control circuit using a proportional integrative controller, namely proportional integral (PI) controller. This controller maintains a constant output voltage in the event of a rise or fall in the source voltage. Also, A low-pass filter was designed to reduce the ripple factor in the output voltage and current.

## 2. METHOD

The Society of Electric Vehicle Engineers has classified three levels of charging for electric vehicles. In the first level, which is considered the slowest in the charging process, a plug is used to connect the charger on board electric vehicle to the port at home. This type of charging is used by people who travel distances of less than 60 kilometers per day, and the vehicle is charged at night at home. In the second level, devices dedicated to the charging of electric vehicles at home or in public stations are used to provide electrical energy of 220 or 240 volts and up to 30 amps. The third level of charging is called direct current (DC) fast charging, in which the charger is located outside the electric vehicle (off-board) in order to reduce the cost, size and weight of the vehicle, where the charging power reaches 90 kW at a charging voltage of 200/450 volts, thereby reducing the charging time to 20-30 minutes [15].

In this paper, a third-level DC fast charger using six pulses fully controlled was designed and built. This research paper is divided into five sections as: the section 1 presents the configuration of the charging station; the section 2 describes the modelling of the charging station; the section 3 is about the control system, which is divided into two parts, namely, an open control circuit and a closed control circuit; the section 4 deals with how to treat the output voltage and reduce the ripple factor in the charger, and in the last section, the results obtained will be presented and discussed.

### 2.1. Configuring the charging station

In this section, a three-phase charger with six pulses was designed using a thyristor. The three-phase charger consisted of a three-phase power source, a step-down transformer, and a voltage converter for converting the alternating current to a direct current before charging the batteries of the electric vehicle. Figure 1 is an illustration of the charger.

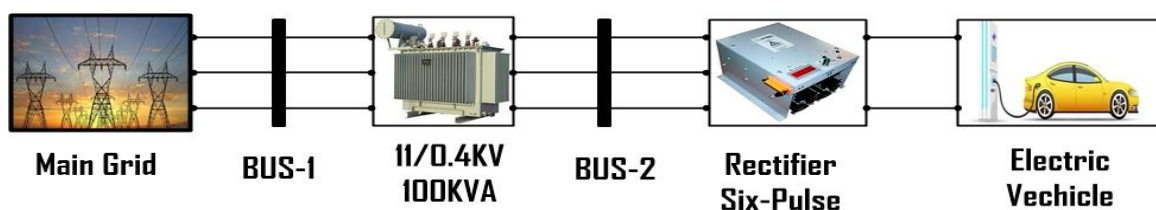


Figure 1. Charging component diagram

**2.2. Modelling of the charging station**

This section involves the modelling of each part of the charging station. The charging station is generally composed of an 11 kV three-phase source, an 11/0.4 KV step-down transformer, three-phase controlled rectifiers and a connected load representing the electric vehicle. Figure 2 shows the configuration of the three-phase rectifier, which comprised three legs, with each leg containing two switches.

The switches were also divided into two groups. The first group was responsible for rectification the positive part of the wave (T1, T3, T5), while the second group was responsible for rectification the negative part of the wave (T2, T4, T6). These switches were operated by applying a short pulse to the thyristor base (GATE), which was then extinguished naturally or by a special extinguishing circuit. The conduction period for each switch was 120 degrees, with 60 degrees being between each switch and the last. The firing of the thyristors was as follows for each switch. If the first switch (T1) was cut at an angle of  $(30+\alpha)$ , then, switch number three (T3) would be cut at an angle of  $(30+\alpha+120)$ , and the fifth switch (T5) would be cut at an angle of  $(30+\alpha+240)$ . The second group was: the fourth switch (T4) was cut at an angle of  $(30+\alpha+180)$ , and the sixth switch (T6) at an angle of  $(30+\alpha+120+180)$ . Finally, the second switch (T2) was cut at an angle of  $(30+\alpha+240+180)$ . The output voltage from the controlling rectifier was given as in (1). Table 1 shows the relationship between the firing angle and conduction angle of each electronic switches [17], [23].

While (1) represents the relationship of the firing angle ( $\alpha$ ) with the output voltage. Also, the Figure 3 represents the output voltage with firing angle. The three-phase rectifier was modelled using MATLAB software, as shown in Figure 4.

$$V_o = \frac{1}{\pi/3} \int_{\frac{\pi}{3}+\alpha}^{\frac{2\pi}{3}+\alpha} Vm_{L-L} \sin(\omega t) d(\omega t) = \frac{3Vm_{L-L}}{\pi} \cos(\alpha) \tag{1}$$

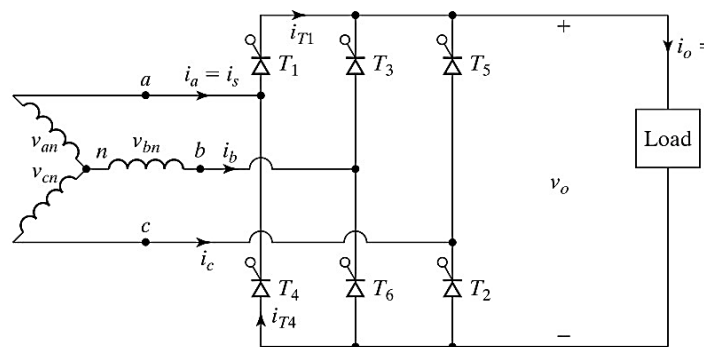


Figure 2. Three phase full wave rectifier [17]

Firing Angle	T1	T2	T3	T4	T5	T6
0°	30°	90°	150°	210°	270°	330°
30°	60°	120°	180°	240°	300°	360°
60°	90°	150°	210°	270°	330°	390°
90°	120°	180°	240°	300°	360°	420°

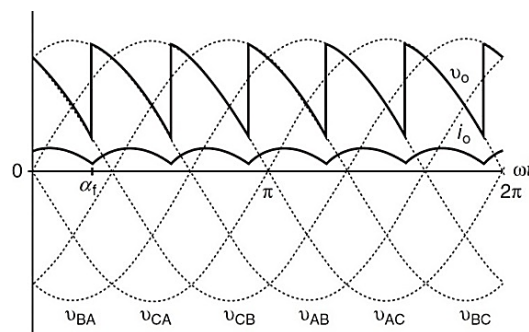


Figure 3. Output voltage at  $\alpha=45^\circ$  [23]

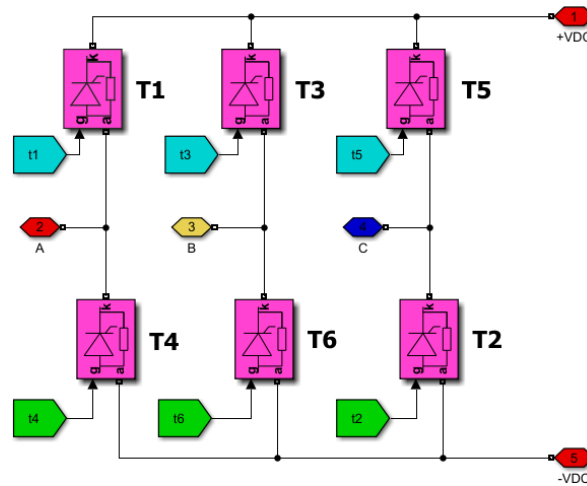


Figure 4. Modeling of three phase full wave control rectifier

The electric vehicle was represented by a load connected to the charger. This was modelled by a battery made up of three components, namely,  $RLV$  [16], [17], [24], [25] where  $R$  represents the internal resistance which determines the value of the charging current,  $L$  represents a small inductance value, and  $V$  (batt) represents the voltage of the battery. Figure 5 shows the model for the battery.

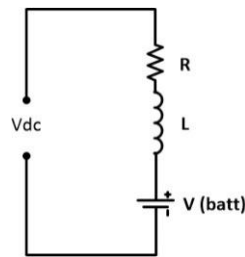


Figure 5. Battery model

### 2.3. Rectifier control circuit

Electronic switches must be fired to obtain a voltage at the output side. These switches can be triggered in a three-phase rectifier circuit by applying pulses to the base of the thyristor, which will thus be biased forward to start the conduction. These pulses are obtained through a pulse generator, where microcontrollers can be practically used to obtain these pulses. It is also possible to obtain these pulses through computer programs such as MATLAB and others that simulate these circuits. In this paper, these pulses were obtained through a simulation of the control circuit. Two types of controls can be implemented, namely, an open-loop control circuit, and a closed-loop control circuit using a proportional integrative controller. The open-loop control circuit shown in Figure 6 is an important circuit for generating the necessary pulses to fire the electronic switches (thyristors).

The pulses generation circuit in Figure 6 consists of a pulse generator, 3-phase-locked loop (3-PLL), and firing angle ( $\alpha$ ). The pulse generator generates the pulses according to the input, while the output is (0, 1), which are then sent to the thyristors. The first input is the firing angle in degrees, and the second input (wt) is the first phase angle (A) in rad, which is obtained from the 3-PLL synchronization system. The last entry is used to block the switches (thyristor) if the input is equal to one.

The second component of the pulse's generation circuit is (3-phase-locked loop 3-PLL). Phase-locked loop technology is a common method for retrieving information on the frequency and angle of electrical systems. The basic idea of a phase-locked loop is its ability to generate a sinusoidal signal whose phase is coherent, following the fundamental component of the input [26]. It is used in power systems, power electronics systems, generating of thyristor firing angles, and for high performance in inverters [27]. A phase-locked loop circuit consists of a voltage-controlled oscillator (VCO), a proportional integral (PI) controller, and a phase detector (PD) [22]. Figure 7 shows the components of a phase-locked loop circuit.

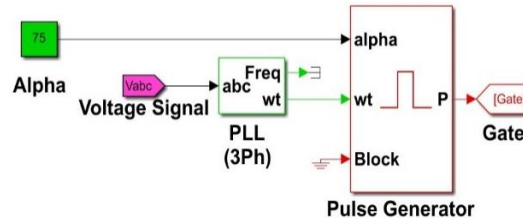


Figure 6. Open loop-pulse generation

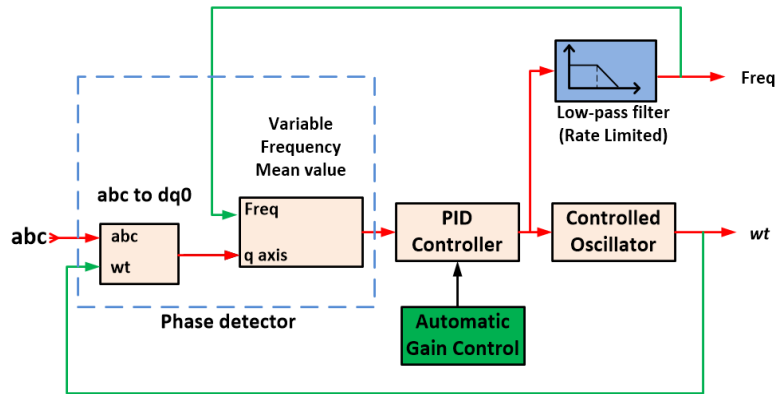


Figure 7. Phase-locked loop components

The input of a Phase-Locked loop circuit is a three-phase voltage, and these three phase signals are converted from the (abc) system to the rotating frame (dq0) using Park’s transformation, where the outputs for this circuit are the frequency and angular [27], [28],  $V_a$ ,  $V_b$ , and  $V_c$  represent the input voltages to the 3-PLL.

$$V_a = V_m \sin(\omega t) \tag{2}$$

$$V_b = V_m \sin(\omega t - \frac{2\pi}{3}) \tag{3}$$

$$V_c = V_m \sin(\omega t - \frac{4\pi}{3}) \tag{4}$$

Park’s transformation equations are used to transform the three-phase system into a rotating reference frame system, as shown (5):

$$\begin{bmatrix} vd \\ vq \end{bmatrix} = \frac{2}{3} \begin{bmatrix} \cos(\theta) & \cos(\theta - \frac{2\pi}{3}) & \cos(\theta + \frac{2\pi}{3}) \\ -\sin(\theta) & -\sin(\theta - \frac{2\pi}{3}) & -\sin(\theta + \frac{2\pi}{3}) \end{bmatrix} \tag{5}$$

where  $\theta$  is represents the angle between d-axis of rotating reference frame and three phase a-axis, and  $vd$  is represents the direct axis reference voltage,  $vq$  is represents the quadrature reference voltage. where the angle ( $\theta$ ) contributes to obtaining the voltages of the rotating frame  $vd$ ,  $vq$ . The  $vq$  is used to obtain the frequency and angular velocity. This voltage is proportional to the phase difference between the input signal (abc) and the rotational frame of the internal oscillator (VCO).

The PID controller in phase locked loop keeps the phase difference value at “zero”, while the frequency value is obtained from the output of the controller (PID) through a low-pass filter. Then, the integrator output of the controller is taken to obtain the angular velocity. However, this method is considered as an open-loop control method in the sense that if there is a change in the input voltage, the output will change, thereby leading to a change in the charging current from the required value, and this will have a negative effect on the battery. This can be seen from (1). Therefore, to avoid this problem, the control circuit must be modified to contain a closed Loop, so that the reference value of the required current is compared

with the current drawn by the battery, in order to generate the appropriate firing angle to maintain a constant charging current. In the closed-loop control circuit, the integrative proportional controller is added to correct the error in order to obtain suitable firing angles to maintain a constant current and voltage to achieve the fast-charging process. This control is used to generate the necessary pulses to trigger the thyristors. Figure 8 shows a closed-loop control circuit. The PI controller used in the circuit shown in Figure 8 can be represented mathematically as in the (6). Figure 9 represents the proportional integrative controller, where  $K_p$  is the proportional gain constant, and  $K_i$  is the integral gain constant.

$$G_{pi}(s) = K_p + K_i/s \tag{6}$$

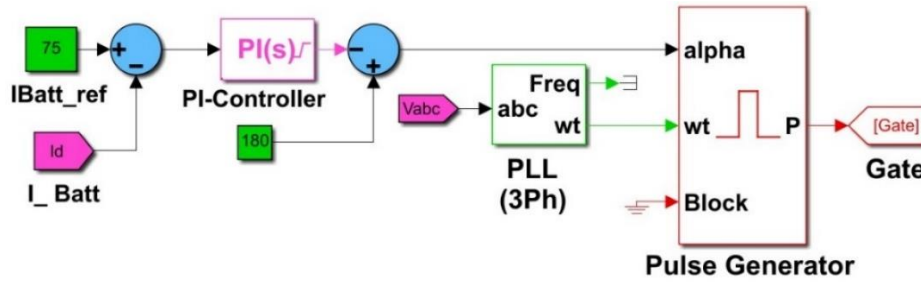


Figure 8. Close loop-pulse generation

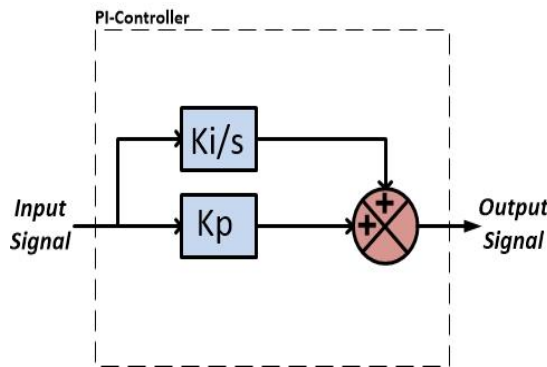


Figure 9. PI controller

The principle of operation of the close-loop controller shown in Figure 8 is as, the output current is compared to the reference current to obtain the error that must be corrected to reach the required value. This error is entered into the PI controller to obtain the connection angle, which is then subtracted from 180 degrees to obtain the firing angle. This is entered into the pulse generator, and then into the switches (thyristors) to be fired to obtain the required voltage. Although the required output voltage is obtained, the output voltage and current contain a high ripple factor if no filter was used, which must be reduced.

**2.4. Output DC smoothing**

When converting an alternating current (AC) voltage to direct current (DC), the DC output voltage will contain an unwanted AC component in the output wave, and this will create a ripple in the DC output voltage. The ripple factor can be defined as the ratio of the root mean square (RMS) value of the ripple voltage ( $V_{rms}$ ) to the direct output voltage ( $V_{dc}$ ). For most applications that use rectifiers, the ripple factor must be within the permissible limit. If the ripple factor is greater than the permissible value, it will have a negative impact on the equipment [23]. A ripple in the output voltage or the charging current will lead to an increase in the temperature of the battery cells, aging, increased losses, skin effect phenomenon, and interference with the frequencies of neighboring communication [29], [30] worth noting that the ripple frequency in the output voltage is equal to the product of the source frequency multiplied by the number of pulses of the rectifier [31].



The ripple factor can be reduced in several ways including: i) increasing the number of pulses for the rectifiers from six to twelve. As the number of pulses increases, the ripple factor will decrease [31], [32]; and ii) using filters on the output side, where a capacitor is connected in parallel with the load to smooth the voltage, and an inductance is connected in series with the load to smooth the current [33]–[35]. Figure 10 shows how the filter was attached to the output side.

The values of the capacitance and inductance were obtained by analyzing the output wave of the voltage or current. An analysis of the fast Fourier transform was carried out, and the frequency of the more influential value was taken and considered as the cut-off frequency of the filter, where the filter was designed so that an electrical resonance occurred at this frequency. To achieve this situation, the value of the ohmic capacitance must be equal to the ohmic inductive ( $X_L=X_C$ ), and the values of the capacitance and inductance were chosen on this basis [16]. The ripple coefficient can be obtained from the (7), while (8) represents the particular equation for finding filter parameters values. This equation was derived from  $X_L=X_C$ . The filter was modelled with the rectifier and electric vehicle as in Figure 11.

$$RF = \sqrt{\left(\frac{V_{rms}}{V_{dc}}\right)^2 - 1} \tag{7}$$

$$L_f = \frac{1}{(2\pi \cdot f_c)^2 \cdot C_f} \tag{8}$$

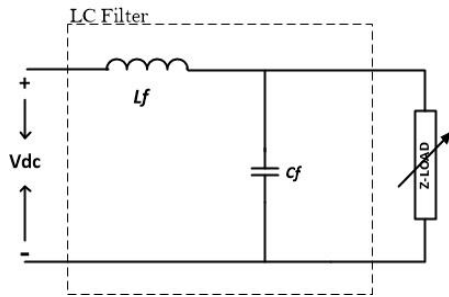


Figure 10. Low pass filter

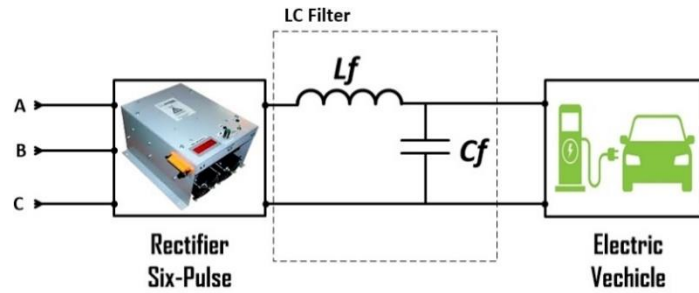


Figure 11. Low pass filter connected with electric vehicle

### 3. RESULTS AND DISCUSSION

In this section, the design proposed in the previous sections was modelled using the MATLAB R2021b program. Table 2 represents the input parameters of the charger that was described in Figure 1. Two cases were considered. The first case involved the modelling of the charger with an open-loop control without and with the use of the filter, and the presentation of the results, while the second case was the modelling of the charger with a closed-loop control with the use of the filter, and the presentation of the results.

The battery charger was implemented as shown in Figure 4. The modelling of the battery is shown in Figure 5 and Table 2. The transformer was implemented directly from the SIMPOWER library, three-phase, two-winding, according to Table 2. Finally, the three-phase source was implemented from Table 2, and the model was finally designed using MATLAB/Simulink, as shown in Figure 1. Before running the model, it was necessary to use the integrative solution method, ode23t, in MATLAB to ensure that the model was accurate and worked well. The first case: the open-loop control circuit Without using a low pass filter. Figure 12 shows the output voltage and current for this case without the use of a filter at the output side.

Parameters	Value
Supply voltage (L-L)	11 kv
Supply frequency	50 Hz
Three phase transformer D/Yn	100 KVA, 50 Hz, 11/0.4 Kv
Charging output voltage and current	450 V, 75 A
load (electric car battery RLV)	300 V, 50 A, 2 Ω, 10 mH

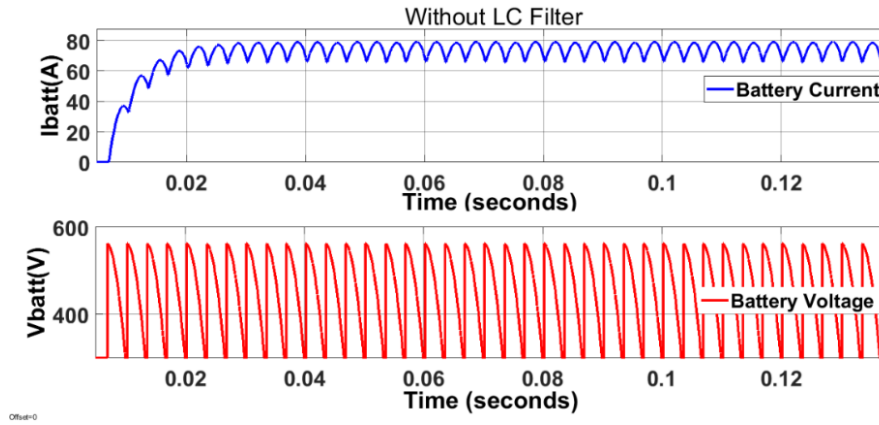


Figure 12. Output current and voltage without low pass filter

From the figure, it can be seen that there was a high amount of ripple in the output current and voltage of the current and voltage. As mentioned in the previous section, this is unacceptable and must be reduced by using a low-pass filter at the output side. In order for the low-pass filter to be designed, a rapid real-time analysis of the current and voltage waveforms shown in Figure 12 must be performed. Furthermore, to obtain the cut-off frequency of the filter that will be used to reduce the ripple in the voltage and current, the analysis was carried out using the current waveform rapid analysis as in Figure 13.

The presence case with filter. The filter is designed with a cut-off frequency of 300 vibrations/sec ( $6 \times 50$ ) as shown in Figure 13. The value of the inductance used in the low-pass filter is found by selecting the capacitive value so that it is feasible. On the basis of it, the inductance value of the coil is calculated through (8). Table 3 represents the capacitance and inductance values of the filter used. After adding the filter to the circuit, as shown in Figure 11, the results shown in Figure 14 were obtained.

From Figure 14 it can be seen that the ripple for the output current and voltage become very small compared to the first case. This shows the importance of adding a low pass filter to the output side to reduce the ripple factor in the output voltage and current. Although the output voltage and current may be free of the ripple factor, the open control circuit does not solve the problem that occurs in the output voltage and current in the event of a decrease or increase in the input voltage. After eliminating the ripples in the current and voltage waves, the open-loop control circuit still suffers from a problem, which is that with the change in the input voltage, it is also accompanied by a change in the output voltage. Thus, the output current required to charge the battery changes. Figure 15 represents the change in the input voltage and the response of the open control circuit.

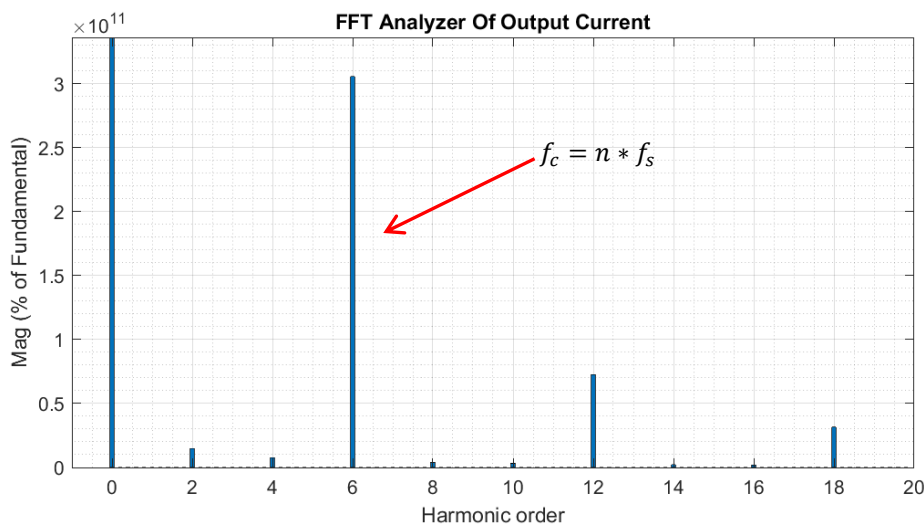


Figure 13. FFT of output current



Table 3. Value of capacitance and inductance

Elements	Value
Capacitance	200 mF
Inductance	1.4072 $\mu$ H

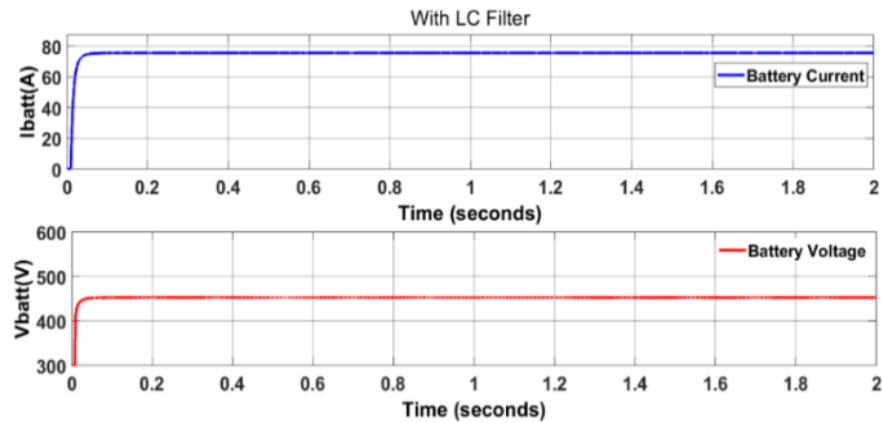


Figure 14. Output current and voltage with low pass filter

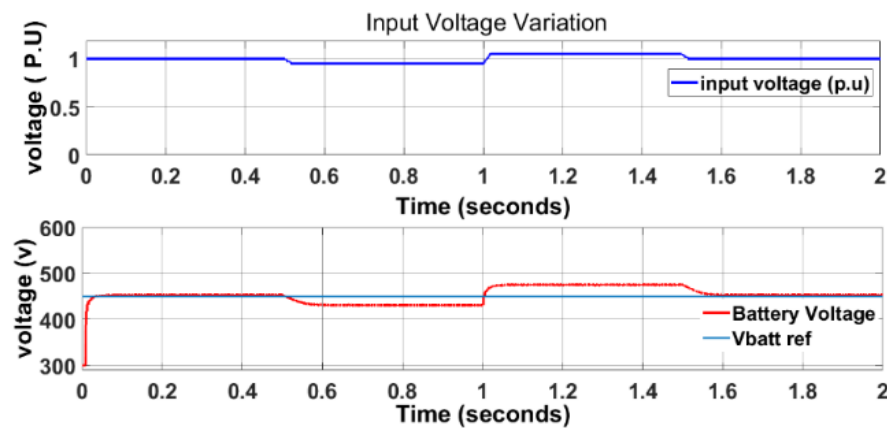


Figure 15. Output voltage with input voltage variation

From Figure 15 it can be seen that if the input voltage is reduced by 5%, which is equivalent to 0.95 P.U. in 0.5 sec, the output voltage will also decrease proportionally to 430 V and it will remain constant at this value. When the input voltage is increased by 0.5% in 1 second, which is equivalent to 1.05 P.U., the value of the output voltage will increase to 475 V. Thus, in an open-loop control circuit, the circuit needs to be adjusted to maintain a constant output current and voltage. In the second case, which simulates a closed-loop control circuit. In this case, the closed control circuit shown in Figure 9 was used, where the gains for the PI controller were obtained by trial-and-error method, and the values that provided a good response to the system were  $K_P=2.15$ , and  $K_i=35.46$ . Figure 16 shows the output current and voltage when the closed-loop control circuit was used. Figure 17 shows the response of the closed-loop control circuit in the event of an increase or decrease of 5% in the input voltage.

Figure 17 shows the importance of using a closed control circuit to maintain the output voltage despite changes to the input voltage, and this will be reflected positively in the charging process. Figure 17 shows that if the input voltage is reduced by 5%, which is equivalent to 0.95 P.U., the output voltage will pass through a transient state within 0.1 second, and the output voltage will return to the reference value of 450 V. Likewise, if the voltage is increased to 1.05 P.U., then the output voltage will return to be equal to the reference voltage. Through the results, it is clear that the closed control circuit maintains the output voltage and current constant when the input voltage changes, unlike the open loop control circuit.

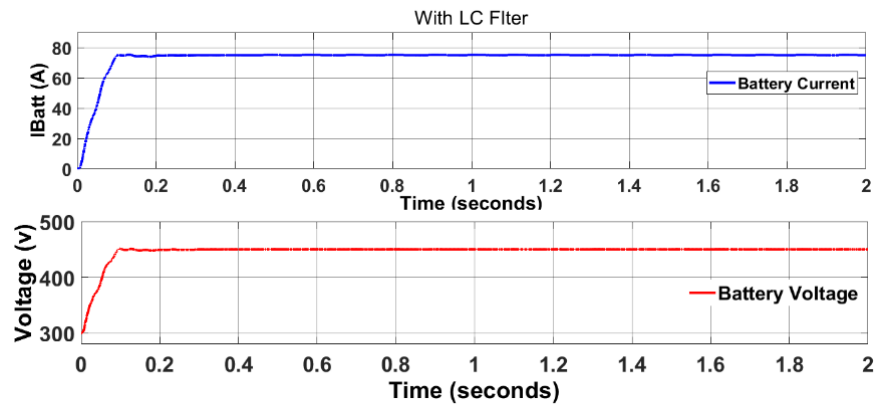


Figure 16. Output current and voltage with close loop control

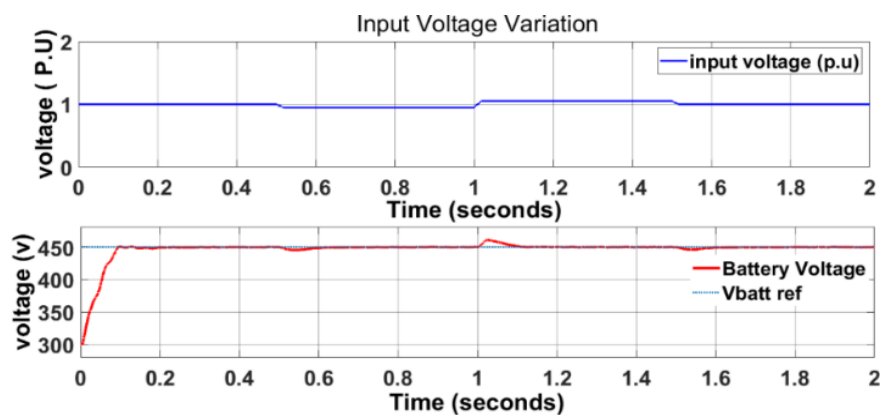


Figure 17. Output voltage with input voltage variation

#### 4. CONCLUSION

In this paper, a new model of a DC fast-charging station with a constant charging current and voltage was designed. An explanation was provided for each component of the charger. In addition to an adequate explanation of the control system, the modelling of the charger was explained in a didactic manner to allow for further research on the topic. The charger was modelled and simulated using MATLAB/Simulink. The case of a charger with an open control circuit was simulated with changes to the input voltage. It was concluded that this type of control is inefficient, especially with sensitive applications such as battery charging operations for electric vehicles. Whereas, when the input voltage is increased by 5%, the output voltage becomes 470 volts and remains constant at this value. Likewise, when the input voltage is reduced by the same amount, the output voltage becomes 430 volts, which affects the charging process of the electric vehicle. Thus, a closed control circuit was designed to obtain a constant current and voltage at the output side. The closed control circuit was simulated, where the simulation results were influenced by changes to the input voltage. When the input voltage was increased or decreased by 5%, this control maintained the value of the current and voltage at the output to be equal to the reference values required to achieve fast charging. Through this process, the battery life was preserved and the charging process was achieved within the scheduled time.

#### ACKNOWLEDGEMENTS

The authors would like to thank University of Mosul, College of Engineering, Electrical Department, for the support given during this work.

#### REFERENCES




- [1] R. Kumar and D. Saxena, "Impact of plug-in electric vehicles on faulted distribution system," *Arabian Journal for Science and Engineering*, vol. 45, no. 3, pp. 1599–1614, Mar. 2020, doi: 10.1007/s13369-019-04104-1.

- [2] L. P. Fernandez, T. G. S. Roman, R. Cossent, C. M. Domingo, and P. Frias, "Assessment of the impact of plug-in electric vehicles on distribution networks," *IEEE Transactions on Power Systems*, vol. 26, no. 1, pp. 206–213, Feb. 2011, doi: 10.1109/TPWRS.2010.2049133.
- [3] D. Doerffel and S. A. Sharkh, "System modeling and simulation as a tool for developing a vision for future hybrid electric vehicle drivetrain configurations," in *2006 IEEE Vehicle Power and Propulsion Conference*, Sep. 2006, pp. 1–6, doi: 10.1109/VPPC.2006.364315.
- [4] J. Y. Yong, V. K. Ramachandaramurthy, K. M. Tan, and N. Mithulananthan, "A review on the state-of-the-art technologies of electric vehicle, its impacts and prospects," *Renewable and Sustainable Energy Reviews*, vol. 49, pp. 365–385, 2015, doi: 10.1016/j.rser.2015.04.130.
- [5] Z. Darabi and M. Ferdowsi, "Aggregated impact of plug-in hybrid electric vehicles on electricity demand profile," *IEEE Transactions on Sustainable Energy*, vol. 2, no. 4, pp. 501–508, Oct. 2011, doi: 10.1109/TSTE.2011.2158123.
- [6] S. F. Tie and C. W. Tan, "A review of energy sources and energy management system in electric vehicles," *Renewable and Sustainable Energy Reviews*, vol. 20, pp. 82–102, Apr. 2013, doi: 10.1016/j.rser.2012.11.077.
- [7] A. König, L. Nicoletti, D. Schröder, S. Wolff, A. Waclaw, and M. Lienkamp, "An overview of parameter and cost for battery electric vehicles," *World Electric Vehicle Journal*, vol. 12, no. 1, Feb. 2021, doi: 10.3390/wevj12010021.
- [8] S. Eaves and J. Eaves, "A cost comparison of fuel-cell and battery electric vehicles," *Journal of Power Sources*, vol. 130, no. 1–2, pp. 208–212, 2004.
- [9] S. Aggarwal and A. K. Singh, "Impact analysis of electric vehicle charging station integration with distributed generators on power systems," *International Journal of Circuit Theory and Applications*, vol. 49, no. 6, pp. 1811–1827, Jun. 2021, doi: 10.1002/cta.2974.
- [10] N. O. Kapustin and D. A. Grushevenko, "Long-term electric vehicles outlook and their potential impact on electric grid," *Energy Policy*, vol. 137, Feb. 2020, doi: 10.1016/j.enpol.2019.111103.
- [11] S. Deb, K. Kalita, and P. Mahanta, "Review of impact of electric vehicle charging station on the power grid," in *2017 International Conference on Technological Advancements in Power and Energy (TAP Energy)*, Dec. 2017, vol. 1, pp. 1–6, doi: 10.1109/TAPENERGY.2017.8397215.
- [12] B. Marah, Y. R. Bhavanam, G. A. Taylor, and A. O. Ekwue, "Impact of electric vehicle charging systems on low voltage distribution networks," in *2016 51st International Universities Power Engineering Conference (UPEC)*, Sep. 2016, pp. 1–6, doi: 10.1109/UPEC.2016.8114052.
- [13] J. G. -Guarin, W. Infante, J. Ma, D. Alvarez, and S. Rivera, "Optimal scheduling of smart microgrids considering electric vehicle battery swapping stations," *International Journal of Electrical and Computer Engineering (IJECE)*, vol. 10, no. 5, pp. 5093–5107, Oct. 2020, doi: 10.11591/ijece.v10i5.pp5093-5107.
- [14] M. A. AL-Yoonus and O. S. Al-deen Alyozbak, "Detection of internal and external faults of single-phase induction motor using current signature," *International Journal of Electrical and Computer Engineering (IJECE)*, vol. 11, no. 4, pp. 2830–2841, Aug. 2021, doi: 10.11591/ijece.v11i4.pp2830-2841.
- [15] F. M. Shakeel and O. P. Malik, "Vehicle-to-grid technology in a micro-grid using DC fast charging architecture," in *2019 IEEE Canadian Conference of Electrical and Computer Engineering (CCECE)*, May 2019, pp. 1–4, doi: 10.1109/CCECE.2019.8861592.
- [16] S. M. Khudher, I. Bin Aris, N. F. Mailah, and R. K. Sahbudin, "Analysis of AC-to-DC uncontrolled converters harmonics for electric vehicles applications," *Pertanika Journal of Science and Technology*, vol. 25, no. S, pp. 283–290, 2017.
- [17] R. Muhammad, K. Narendra, and R. Ashish, "Power electronics: devices, circuits and applications," *Pearson Education*, 2014.
- [18] O. Hegazy, J. Van Mierlo, and P. Lataire, "Control and analysis of an integrated bidirectional DC/AC and DC/DC converters for plug-in hybrid electric vehicle applications," *Journal of Power Electronics*, vol. 11, no. 4, pp. 408–417, Jul. 2011, doi: 10.6113/JPE.2011.11.4.408.
- [19] H. Tu, H. Feng, S. Srdic, and S. Lukic, "Extreme fast charging of electric vehicles: a technology overview," *IEEE Transactions on Transportation Electrification*, vol. 5, no. 4, pp. 861–878, Dec. 2019, doi: 10.1109/TTE.2019.2958709.
- [20] A. K. Verma, B. Singh, and D. T. Shahani, "Grid to vehicle and vehicle to grid energy transfer using single-phase half bridge boost AC-DC converter and bidirectional DC-DC converter," *International Journal of Engineering, Science and Technology*, vol. 4, no. 1, pp. 46–54, Mar. 2018, doi: 10.4314/ijest.v4i1.6S.
- [21] M. Yilmaz and P. T. Krein, "Review of battery charger topologies, charging power levels, and infrastructure for plug-in electric and hybrid vehicles," *IEEE Transactions on Power Electronics*, vol. 28, no. 5, pp. 2151–2169, May 2013, doi: 10.1109/TPEL.2012.2212917.
- [22] A. Arancibia and K. Strunz, "Modeling of an electric vehicle charging station for fast DC charging," in *2012 IEEE International Electric Vehicle Conference*, Mar. 2012, no. 3, pp. 1–6, doi: 10.1109/IEVC.2012.6183232.
- [23] A. Trzynadlowski, "Modern power electronics," *IEEE Power Engineering Review*, vol. 18, no. 7, pp. 31–31, Jul. 1998, doi: 10.1109/MPER.1998.686953.
- [24] A. Sarwar and M. S. J. Asghar, "Multilevel converter topology for solar PV based grid-tie inverters," in *2010 IEEE International Energy Conference*, Dec. 2010, pp. 501–506, doi: 10.1109/ENERGYCON.2010.5771733.
- [25] R. Saadi *et al.*, "Energy management of fuel cell/ supercapacitor hybrid power sources based on the flatness control," in *4th International Conference on Power Engineering, Energy and Electrical Drives*, May 2013, pp. 128–133, doi: 10.1109/PowerEng.2013.6635593.
- [26] M. Karimi-Ghartemani and M. R. Iravani, "A new phase-locked loop (PLL) system," in *Proceedings of the 44th IEEE 2001 Midwest Symposium on Circuits and Systems. MWSCAS 2001 (Cat. No.01CH37257)*, 2001, vol. 1, pp. 421–424, doi: 10.1109/MWSCAS.2001.986202.
- [27] A. M. Salamah, S. J. Finney, and B. W. Williams, "Three-phase phase-lock loop for distorted utilities," *IET Electric Power Applications*, vol. 1, no. 6, 2007, doi: 10.1049/iet-epa:20070036.
- [28] Y. Levron and J. Belikov, "Modeling power networks using dynamic phasors in the dq0 reference frame," *Electric Power Systems Research*, vol. 144, pp. 233–242, Mar. 2017, doi: 10.1016/j.epsr.2016.11.024.
- [29] S. De Breucker, K. Engelen, R. D'hulst, and J. Driesen, "Impact of current ripple on li-ion battery ageing," *World Electric Vehicle Journal*, vol. 6, no. 3, pp. 532–540, Sep. 2013, doi: 10.3390/wevj6030532.
- [30] K. Uddin, A. D. Moore, A. Barai, and J. Marco, "The effects of high frequency current ripple on electric vehicle battery performance," *Applied Energy*, vol. 178, pp. 142–154, Sep. 2016, doi: 10.1016/j.apenergy.2016.06.033.
- [31] M. Mazaheri, V. Scaini, and W. E. Veerkamp, "Cause, effects, and mitigation of ripple from rectifiers," *IEEE Transactions on Industry Applications*, vol. 39, no. 4, pp. 1187–1192, Jul. 2003, doi: 10.1109/TIA.2003.813728.




- [32] B. Singh, G. Bhuvaneswari, V. Garg, and S. Gairola, "Pulse multiplication in AC–DC converters for harmonic mitigation in vector-controlled induction motor drives," *IEEE Transactions on Energy Conversion*, vol. 21, no. 2, pp. 342–352, Jun. 2006, doi: 10.1109/TEC.2006.874217.
- [33] J. G. Cho, C. Y. Jeong, J. W. Baek, D. I. Song, D. W. Yoo, and C. Y. Won, "High power factor three phase rectifier for high power density AC/DC conversion applications," in *APEC '99. Fourteenth Annual Applied Power Electronics Conference and Exposition. 1999 Conference Proceedings (Cat. No.99CH36285)*, 1999, vol. 2, pp. 910–915, doi: 10.1109/APEC.1999.750476.
- [34] Y. Liu, M. Huang, H. Wang, X. Zha, J. Gong, and J. Sun, "Reliability-oriented optimization of the LC filter in a buck DC-DC converter," *IEEE Transactions on Power Electronics*, vol. 32, no. 8, pp. 6323–6337, Aug. 2017, doi: 10.1109/TPEL.2016.2619690.
- [35] J. Kim, J. Choi, and H. Hong, "Output LC filter design of voltage source inverter considering the performance of controller," in *PowerCon 2000. 2000 International Conference on Power System Technology. Proceedings (Cat. No.00EX409)*, 2000, vol. 3, pp. 1659–1664, doi: 10.1109/ICPST.2000.898225.

## BIOGRAPHIES OF AUTHORS






**Wisam Mohamed Najem**    he obtained his Bachelor of Science (BSc) in Electrical Engineering in 2012 from the Electrical Engineering Department, College of Engineering, University of Mosul, Iraq. Now he is a master's student at the same university mentioned above, in the field of studying the effect of electric vehicle charging stations on power systems protection. He can be contacted at: wisam.20enp50@student.uomosul.edu.iq.



**Omar Sh. Alyozbaky**    he obtained his Bachelor of Science (B.Sc.) in Electrical Engineering in 2001 from the Electrical Engineering Department, College of Engineering, University of Mosul, Iraq. Then he was appointed as an assistant engineer in the same mentioned department. After that, he got MSc in "Overcome the effect of critical distance in XLPE high voltage cables by inductive shunt compensator," 2008 from the same mentioned department as well. Upon his graduation, he was appointed as teaching staff (assistant lecturer) in the Electrical Engineering Department, College of Engineering, University of Mosul. In 2012, he obtained the scientific title (lecturer) and the Ph.D. degree in the Department of Electrical and Electronic Engineering, Faculty of Engineering, University Putra Malaysia in 2017. Since 2014, he was a member of the Centre for Electromagnetic and lightning protection research (CELP). Now, he is Assistant Professor Electrical Engineering Department, College of Engineering, University of Mosul. The subjects for interest, renewable energy fields associated with the smart grid, electric vehicles, thermal modeling transformer design, and electrical machines. He can be contacted at email: o.yehya@uomosul.edu.iq, o.sh.alyozbaky@gmail.com.



**Shaker M. Khudher**    he obtained his Bachelor of Science (BSc) in Electrical Engineering in 2001 from the Electrical Engineering Department, College of Engineering, University of Mosul, Iraq. Then he got MSc in "Transmission line distance protection using artificial neural network," 2006 from the same mentioned department. In 2007 he was appointed as teaching staff (assistant lecturer) in the Electrical Engineering Department, College of Engineering, University of Mosul. He obtained the Ph.D. degree in the Department of Electrical and Electronic Engineering, Faculty of Engineering, University Putra Malaysia in 2019. Now, he is a Lecturer at Electrical Engineering Department, College of Engineering, University of Mosul. The subjects for interest, power system analysis and protection, renewable energy fields associated with the smart grid, electric vehicles charging stations. He can be contacted at email: shakeralhyane@uomosul.edu.iq.